The Influence of Mechanical and Thermal Forcing by the Tibetan Plateau on Asian Climate

GUOXIONG WU,* YIMIN LIU,* TONGMEI WANG,*,+ RIJIN WAN,*,+ XIN LIU,# WEIPING LI,@ ZAIZHI WANG,@ QIONG ZHANG,* ANMIN DUAN,* AND XIAOYUN LIANG@

*State Key Laboratory of Numerical Modeling for Atmospheric Sciences and Geophysical Fluid Dynamics, Institute of Atmospheric Physics, Chinese Academy of Sciences, Beijing, China
+ Graduate University of Chinese Academy of Sciences, Beijing, China
# Institute of Tibetan Plateau Research, Chinese Academy of Science, Beijing, China
@ National Climate Center, China Meteorological Administration, Beijing, China

(Manuscript received 11 May 2006, in final form 1 December 2006)

ABSTRACT

This paper attempts to provide some new understanding of the mechanical as well as thermal effects of the Tibetan Plateau (TP) on the circulation and climate in Asia through diagnosis and numerical experiments. The air column over the TP descends in winter and ascends in summer and regulates the surface Asian monsoon flow. Sensible heating on the sloping lateral surfaces appears from the authors' experiments to be the major driving source. The retarding and deflecting effects of the TP in winter generate an asymmetric dipole zonal-deviation circulation, with a large anticyclone gyre to the north and a cyclonic gyre to the south. Such a dipole deviation circulation enhances the cold outbreaks from the north over East Asia, results in a dry climate in south Asia and a moist climate over the Indochina peninsula and south China, and forms the persistent rainfall in early spring (PRES) in south China. In summer the TP heating generates a cyclonic spiral zonal-deviation circulation in the lower troposphere, which converges toward and rises over the TP. It is shown that because the TP is located east of the Eurasian continent, in summertime the meridional winds and vertical motions forced by the Eurasian continental-scale heating and the TP local heating are in phase over the eastern and central parts of the continent. The monsoon in East Asia and the dry climate in middle Asia are therefore intensified.

1. Introduction

The Tibetan Plateau (TP; also Qinghai-Xizang Plateau in China) extends over the area of 27°–45°N, 70°–105°E, covering a region about a quarter of the size of the Chinese territory. Its mean elevation is more than 4000 m above sea level with the 8844-m (near 300 hPa) peak of Mount Everest standing on its southern fringe. The mean TP altitude lies above 40% of the atmosphere. Because of the lower air pressure, various radiation processes over the plateau, particularly in the boundary layer, are quite distinct from those over lower-elevated regions (e.g., Liou and Zhou 1987; Smith and Shi 1992; Shi and Smith 1992). While the TP receives strong solar radiation at the surface, the other parts of Asia at such a level are already in the cold middle troposphere. Geographically the TP is located in the subtropics with westerly winds to the north and easterlies to the south in summer, but it provides a barrier to the subtropical westerly jet in winter. Perturbations forced by the TP can generate Rossby waves in the westerlies, which can propagate downstream and influence the circulation anomaly elsewhere. It is also located over the central and eastern parts of the Eurasian continent, facing the Indian Ocean to the south and the Pacific Ocean to its east. Therefore the Tibetan Plateau can exert profound thermal and dynamical influences on the circulation, energy, and water cycles of the climate system.

Before the 1950s, most of the studies concerning the influence of large-scale topography upon atmospheric circulation and climate focused on its mechanical aspects (Queney 1948; Charney and Eliassen 1949; Bolin 1950; Yeh 1950). In 1957, Yeh et al. (1957) and Flohn

Corresponding author address: Dr. Yimin Liu, State Key Laboratory of Numerical Modeling for Atmospheric Sciences and Geophysical Fluid Dynamics, Institute of Atmospheric Physics, Chinese Academy of Sciences, Beijing 100029, China.
E-mail: lym@lasg.iap.ac.cn

DOI: 10.1175/JHM609.1

(1957), respectively, found that the Tibetan Plateau is a heat source for the atmosphere in summer. Using then available observations, Yeh et al. calculated each term of the heat budget equation and reported that the TP is a weak heat sink in winter but a large heat source in summer. Since then, the temporal and spatial distributions of the heating field over the Tibetan Plateau and their impacts on weather and climate have become an active area of research and many significant results have been achieved.

Recently, Yanai and Wu (2006) gave a thorough review of the past studies about the effects of the TP. The review starts with research from the 1950s on the jet stream, the warm south Asian high, and the early progress of TP research in China. The review then goes over studies concerning the mechanical effects of the TP on large-scale motion, the winter cold surge, and the summer negative vorticity source over the TP. The review also covers the importance of the thermal influences of the TP on the seasonal circulation transition and Asian monsoon onset based on different datasets and numerical experiments (Ye and Gao 1979; Tao and Chen 1987; Wu 2004; Wu et al. 1997a, 2002, 2004; Liu et al. 2001; Liu X. et al. 2001, 2002; Mao et al. 2002a,b; Wang and Lin 2002). Great efforts are made in reviewing the evaluation of the heating source on the TP through the analyses of spatial and temporal distributions of $\langle Q_1 \rangle$ and $\langle Q_2 \rangle$ in the notation used by Yanai et al. (1973) and based on observations from the First Global Atmospheric Research Program (GARP) Global Experiment (FGGE) (December 1978–November 1979) and the Qinghai-Xizang Plateau Meteorology Experiment (QXPMEX) [conducted from May to August 1979 by Chinese meteorologists (Zhang et al. 1988)].

Scientists and visiting scholars at the University of California, Los Angeles (UCLA) headed by Professor M. Yanai evaluated the TP heating source (Yanai et al. 1973, 1992; Yanai and Li 1994; Shen et al. 1984; Liou and Zhou 1987; Nitta 1983; Luo and Yanai 1983, 1984; He et al. 1987) and studied the seasonal changes in the large-scale circulation, thermal structure, and heat sources and moisture sinks over the Tibetan Plateau and the surrounding areas (Yanai et al. 1992). They also employed the global analyses prepared by the European Centre for Medium-Range Forecasts (ECMWF) to study the onset and interannual variability of the Asian summer monsoon in relation to land–sea thermal contrast (Li and Yanai 1996), the Australian summer monsoon (Hung and Yanai 2004), and its relationship with the Asian summer monsoons (Hung et al. 2004).

In China, in the last decade, a series of research programs have been organized to support the activities related to the World Climate Research Programme (WCRP). They were funded by the Chinese Academy of Sciences (CAS), the National Natural Science Foundation of China (NSFC), and the Ministry of Sciences and Technology of China (MOST). The second atmospheric Tibetan Plateau Field Experiment (TIPEX) was organized in 1998 to provide valuable extra in situ observations (Zhou et al. 2000). The publication of the ECMWF and the National Centers for Environmental Prediction–National Center for Atmospheric Research (NCEP–NCAR) (Kalnay et al. 1996) reanalysis datasets provided other important data sources for the relevant study. In addition, the progress of the development of the Global Ocean–Atmosphere–Land System climate model (GOALS) (Wu et al. 1997b; Zhang et al. 2000) at the National Key Laboratory of Numerical Modeling for Atmospheric Sciences and Geophysical Fluid Dynamics (LASG) made numerical experiments available.

Great efforts have been made to understand the mechanism concerning how the TP forcing, either mechanical or thermodynamic, can affect the regional as well as global climate. Some of the results are summarized as one part of this study and can be considered as a complement to the review of Yanai and Wu (2006). In another part of this study, diagnosis and numerical experiments are used to get new insights on our understanding.

The NCEP–NCAR data have an overall intrinsic limit of reliability (Trenberth and Guillemot 1998; Yanai and Tomita 1998; Annamalai et al. 1999; Hung et al. 2004) and should be used with caution. From 1995 to 1999 there was a China–Japan cooperation experiment of surface energy and water cycle over the TP. Six automatic meteorology stations (AMS) were installed at Lhasa (29°40′N, 91°08′E), Rikeze (29°15′N, 88°53′E), Lingzi (29°34′N, 94°28′E), Nagqu (31°29′N, 92°04′E), Gaize (32°09′N, 84°25′E), and Shiquanhe (32°30′N, 80°05′E). Based on these observations, the surface fluxes were calculated by Li et al. (2000, 2001). Duan and Wu (2005) compared the surface sensible heat flux at these six stations with those of NCEP–NCAR at the adjacent grid points. They found that in most cases, the temporal variations in the surface sensible heat flux of the NCEP–NCAR- and AMS-based results are similar on the monthly mean scale at all six stations. The main difference exists in the magnitude. Apart from at Rikeze, the surface sensible heat flux of NCEP–NCAR is always weaker than that based on AMS, which may lead to an underestimation of the impacts of the sensible heat flux on the TP on climate. For the latent heating, by comparing the July mean precipitation fields of the NCEP–NCAR and Xie–Arkin data (Xie and Arkin 1996, 1998) in the same period from 1978 to

1998, Duan and Wu found remarkable differences in East Asia between the two datasets. However, over the TP area, the two datasets possess a similar spatial distribution with decreasing rainfall from the southeastern to northwestern TP and a maximum rainfall center of more than 14 mm day^{-1} over the north of the Bay of Bengal (BOB). For assessing the upper-level routine data, such as geopotential height, temperature, and wind, Duan (2003) compared the NCEP–NCAR with another reanalysis dataset, the Global Energy and Water Cycle Experiment (GEWEX) Asian Monsoon Experiment (GAME) in Intensified Observation Period (IOP) (Tanaka et al. 2001), with the same horizontal resolution (2.5° × 2.5°) and vertical levels during April to October 1998. This latter dataset assimilates the observations from the field experiments TIPEX, the Huaihe River Basin Experiment (HUBEX), the South China Sea Monsoon Experiments (SCSMEX), and GAME-Tibet and some radiosonde as well as wind profile observations from Thailand, India, and Vietnam. The results show that the discrepancy between the two datasets is small for the monthly mean time scale. Therefore in the following diagnoses when NCEP–NCAR reanalysis is employed, we confine ourselves to the investigations of large-scale and long-term monthly mean diabatic heating over the TP and its impacts on large-scale circulations.

This study composes two main parts. The first part presented in section 2 is more theoretical. The air column over the TP descends in winter and ascends in summer each year, working as an air pump and regulating the atmospheric circulation. After discussing the thermal features of the TP, the significance of the surface sensible heating, particularly on its sloping surface, in the effective working of such an air pump is discussed, and the concept of the TP sensible heat driving air pump (TP-SHAP) is further stressed. The seasonal variation of heating over the TP and its impact on the winter and summer circulations in the lower troposphere are also discussed in this part. By analyzing the zonal-deviation wind field at 850 hPa and comparing the results with those from numerical experiments, a wintertime "asymmetric dipole" pattern and a summertime "convergent spiral" pattern of the zonal-deviation flows are obtained. It is shown that the former is mainly due to the mechanical forcing of the TP, whereas the latter is mainly forced by the TP-SHAP. The second part of this study is presented in section 3. Here it is demonstrated how the wintertime dipole-type forcing and the summertime spiral-type forcing of the TP influence the Asian climate. Section 3a focuses on how the mechanical forcing of the TP in late winter and early spring contributes to the occurrence of the persistent rainfall in early spring (PRES) over southern China. Section 3b describes how the summertime continental forcing over Eurasia and the local forcing due to the TP work together to intensify the monsoon in East Asia and the dry climate in middle Asia. A summary and outlook are given in section 4.

2. Theory

a. The Tibetan Plateau sensible heat driving air pump

1) OBSERVATION EVIDENCE

Figure 1a shows the climate-mean seasonal evolutions of the surface sensible heating and the column-integrated total heating over the TP area (27.5°–37.5°N, 80°–100°E) (as shown by the heavy rectangle in Fig. 3). The calculation is based on the 18-yr (1980–97) monthly mean NCEP–NCAR reanalysis. It demonstrates that the TP is a heat sink in the winter months from November to February but a heat source in the summer months from March to October, in agreement with the earliest finding of Yeh et al. (1957; Ye and Gao 1979). Figure 1b shows the seasonal variation of the longitudinal distribution of the surface sensible heat flux averaged from 27.5° to 37.5°N where the TP is located. In winter, while the downward surface sensible heat flux goes from atmosphere to land over the TP region, strong upward sensible heat fluxes are observed over the western Pacific. This is because the frequent wintertime cold outbreaks moving toward the coastal ocean from the Asian continent uptake huge amounts of energy from the underlying ocean surface. In summer, the longitudinal thermal contrast between land and sea is reversed: strong upward surface heating occurs over land, while the heating over the ocean becomes tranquil or even downward. This is because in summertime the subtropical western Pacific Ocean is covered by a stable and warm anticyclone, which effectively suppresses the in situ air–sea interactions. It is so strong that the west–east land–sea thermal contrast across the eastern coast of China (~120°E) is greatly enhanced, and the reversal of the thermal contrast between winter and summer becomes remarkable. These are in favor of the intensification of northerly winds in winter and southerlies in summer over East Asia, contributing to the formation of the strong East Asian monsoon. Furthermore, the Asian monsoon onset is associated with the reversal of the meridional temperature gradient in the upper troposphere along the subtropics (Flohn 1968; Li and Yanai 1996). The earliest reversal occurs over the eastern BOB because the strong heating over the TP in spring can increase the temperature in the northern subtropics earlier than

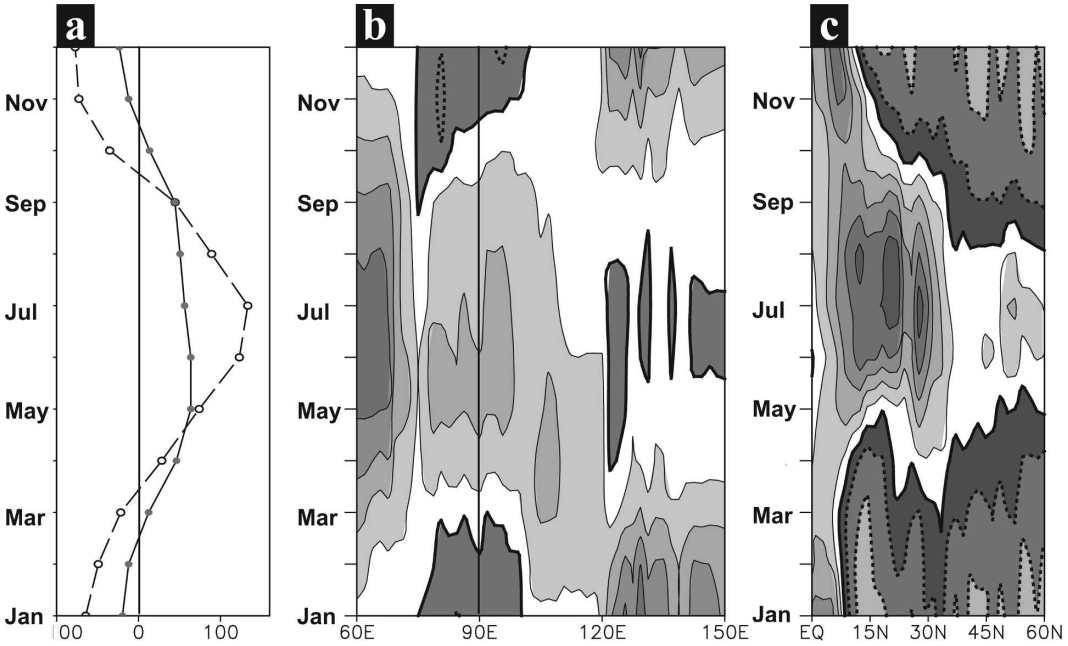

FIG. 1. Seasonal evolutions of (a) column-integrated total heating (dashed curve with open circles) and surface sensible heating (solid curve with solid circles) averaged over TP (27.5°–37.5°N, 80°–100°E); (b) surface sensible heating averaged over 27.5°–37.5°N; and (c) column-integrated total heating averaged over 80°–100°E calculated from the monthly climatology of the NCEP–NCAR reanalysis for 1980–97. Unit is W m^{-2}. Contour interval is 30 W m^{-2} in (b) and 50 W m^{-2} in (c). Values of more than 30 W m^{-2} in (b) and 50 W m^{-2} in (c) are lightly shaded and have thin solid contours, while negative values in (b) and (c) are bounded by heavy solid curves and indicated by heavy shading and dotted contours.

other longitude domains (Wu and Zhang 1998; Mao et al. 2002a,b). The evolution of the 18-yr mean column-integrated total diabatic heating rate averaged between 80° and 100°E (Fig. 1c) shows that before March the heating in this longitude domain is negative everywhere except near the equator. From March onward, the heating over the main part of the TP becomes positive (see also the dashed curve with open circles in Fig. 1a), while the heating over the BOB to its south and over the continental area to its north stays negative till early May when the BOB monsoon onset occurs (Wu and Zhang 1998). This demonstrates again that the TP heating in spring is important for the Asian monsoon onset.

Figure 2 shows the cross sections along 30°N and 90°E of the January (Figs. 2a,c) and July (Figs. 2b,d) mean potential temperature and wind vector projected onto the corresponding cross sections in which the vertical velocity w has been multiplied by 10^3. In January along 30°N (Fig. 2a), cold temperatures over continents and warm temperatures over oceans are prominent. Atmospheric cooling indicated by air descent ($\mathbf{V} \cdot \nabla\theta < 0$) prevails in the free troposphere. Along 90°E (Fig. 2c), the strong cooling is over the TP and its southern slope in association with the strong heating and ascent over the equator. During summer, the warmest center of potential temperature is just over the TP. This is in agreement with the existence of the warm temperature center in July over the plateau (Yanai et al. 1992). Strong ascent prevails in the area to its east from the TP to eastern China (Fig. 2b) and to its south from the TP to the BOB (Fig. 2d), penetrating the isentropic surfaces almost perpendicularly and indicating the existence of a strong heating source over the area in summer (Kuo and Qian 1982; Liu X. et al. 2002; Wu 2004).

Figure 3 shows the deviations from the annual mean of the January and July mean streamlines 10 m above the surface calculated from the NCEP–Department of Energy (NCEP–DOE) Atmospheric Model Intercomparison Project II (AMIP-II) (NCEPII) reanalysis for the period 1979–98. It is evident that the deviation air currents flow from the winter hemisphere into the summer hemisphere and diverge out of continents and converge toward oceans in the midlatitude areas in the winter hemisphere but converge toward the continents and diverge out of oceans in the summer hemisphere. A remarkable circulation reversal appears over the Asian–Australia (A–A) monsoon area. In January the surface air is diverged out of the TP region toward South Africa and Australia in the Southern Hemisphere, whereas in July the surface air is converged into

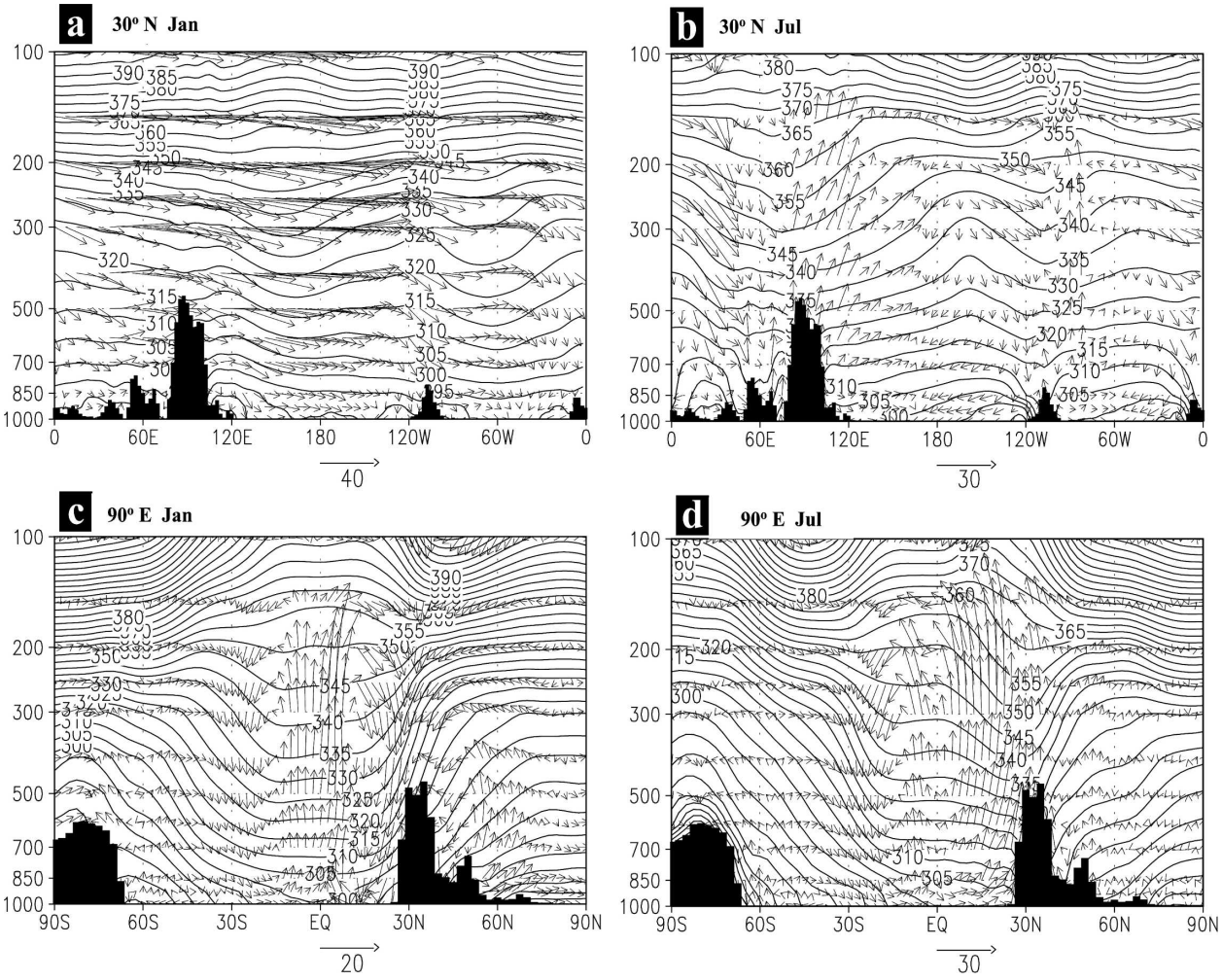

FIG. 2. (left) January and (right) July mean cross sections of potential temperature (contours; interval is 5 K) and vertical circulation (vectors) along 30°N in (a) and (b) and along 90°E in (c) and (d) from NCEP–NCAR reanalysis (1986–95). The shaded area is the in situ vertical profile of orography; from Yanai and Wu (2006).

the TP region from South Africa and Australia, characterizing the seasonal reversal of the A–A monsoon flows.

2) SENSITIVITY NUMERICAL EXPERIMENTS: SUMMER

From Figs. 2 and 3, it looks as if the cooling and descent of the air column above the Tibetan Plateau in winter could account for the surface divergence flow, whereas the heating and ascent of the air column above the TP in summer could explain the surface flow convergence toward the TP area, though the huge heating and ascent south of the TP at the equator (Fig. 2c) can weaken the effect of decent over the TP in winter. In other words the TP air pump above the TP may play significant roles in regulating the A–A monsoon. However, were there no surface sensible heating especially on the sloping surfaces, such a TP air pump as identified from Fig. 2 would not be able to converge/diverge the surface air flows from/into the surrounding areas in the lower layers.

To illustrate the significance of the sensible heating over the sloping surfaces in the operation of the TP air pump, a series of aqua-planet experiments have been conducted based on an atmospheric general circulation model. The model system used in this paper is a new version of the GOALS Spectral Atmospheric Model developed at LASG, Institute of Atmospheric Physics (IAP; GOALS-SAMIL, version R42L9; Wu et al. 2003; Wang et al. 2004). It has 42 rhomboidally truncated spectral waves in the horizontal with resolution equivalent to 2.81° longitude × 1.66° latitude. In the vertical,

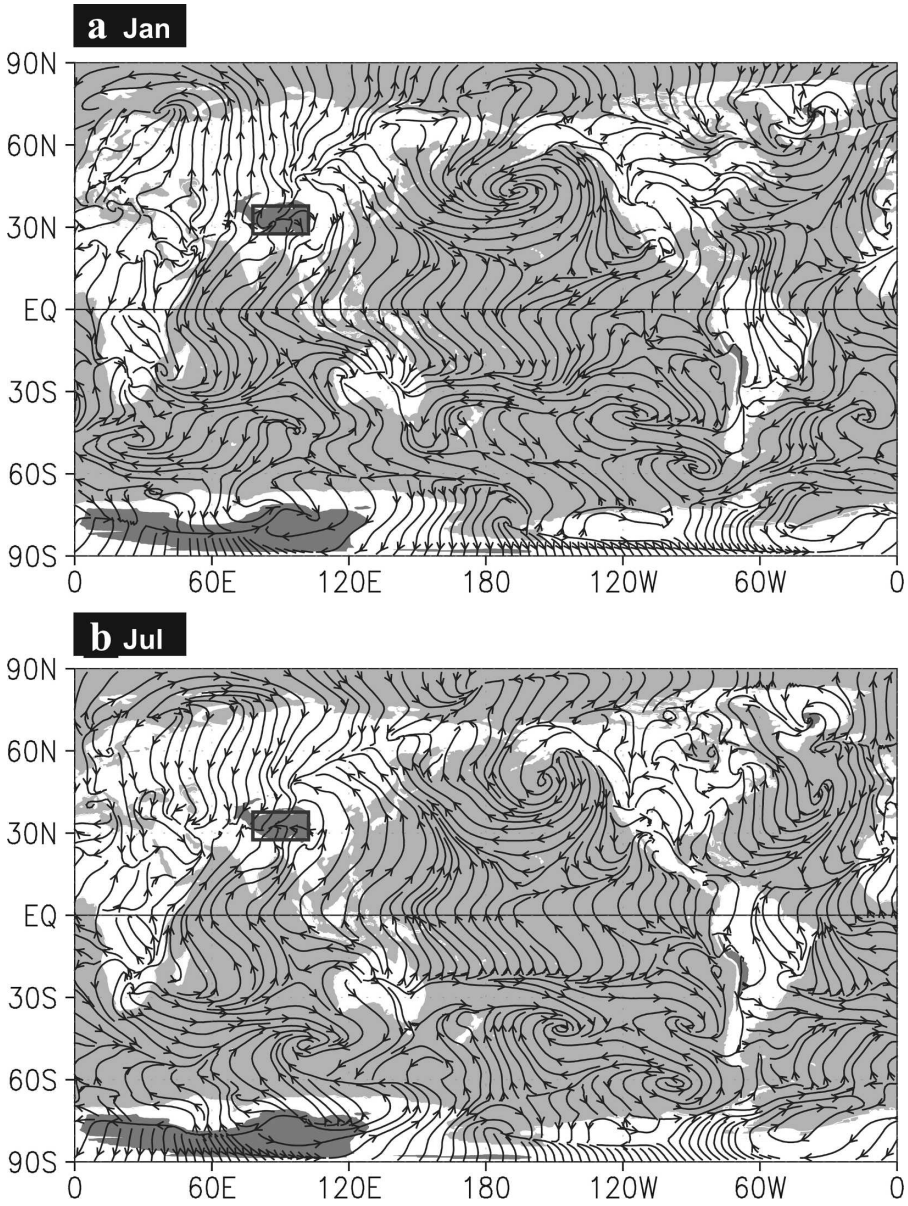

FIG. 3. Distributions of the monthly mean stream field composed of horizontal wind deviations at 10 m from the corresponding annual means of 1979–98 NCEPII reanalysis: (a) January and (b) July. Dark shadings highlight elevations higher than 3000 m. Rectangle indicates the Tibetan Plateau area as defined in the text.

it has nine levels in a σ-coordination system. The model uses a unique dynamical framework by introducing a reference atmosphere and using a semi-implicit time integration scheme (Wu et al. 1997b). The physical processes of the model are quite self-contained, including a K-distribution radiation scheme (Shi 1981), Slingo's cloud diagnosis scheme (Slingo 1987), and the Simplified Simple Biosphere model (SSiB) (Xue et al. 1991; Liu and Wu 1997). For the present purpose, aquaplanet experiments are designed with an idealized topography:

$$h(\lambda, \varphi) = \min\left[3\ \text{km}, h_0 \cos\left(\frac{\pi}{2}\frac{\lambda - \lambda_0}{\lambda_d}\right)\cos\left(\frac{\pi}{2}\frac{\varphi - \varphi_0}{\varphi_d}\right)\right]\begin{bmatrix} -\lambda_d \le \lambda \le \lambda_d \\ (-\varphi_d \le \varphi \le \varphi_d) \end{bmatrix}, \quad (1)$$

being introduced into the "aqua planet" in which the earth's surface in the model is covered merely by ocean. In (1), h is elevation, λ is longitude, φ is latitude, and λ_d and φ_d are the half-width in longitude and latitude, respectively. To mimic the TP, the following parameters are set:

$$\lambda_0 = 90°\text{E}, \quad \varphi_0 = 30°\text{N}, \quad \lambda_d = 40° \text{ longitude},$$
$$\varphi_d = 16.5° \text{ latitude}, \quad \text{and} \quad h_0 = 5 \text{ km}. \tag{2}$$

In addition, a value of 3 km is set for the elevation limit so that a platform, a flat top of the plateau as shown on the left panels in Fig. 4, can be formed. The ground surface is covered by grass alone. Such a treatment on ground type (soil type is 7) can minimize the impact of land–sea thermal contrast and let us concentrate on the influence of the elevated heating over the topography on the circulations. By using such a design, the surface of the topography is divided into two parts: the sloping surface and the platform top surface as demonstrated on the left panels of Fig. 4. In all experiments, the cloud amounts are prescribed by using the climate zonal means (Wu et al. 2004). The solar angle is set on 15 July so that perpetual July experiments are assumed, and the initial fields are taken from the July means of the original model integration. All the integrations are performed for 540 days, and the results averaged from the last 360 days are taken for the following diagnosis.

There are four experiments, that is, NOSH, ALLSH, SLPSH, and TOPSH:

- NOSH: None of the TP surfaces possesses surface sensible heating;
- ALLSH: All of the TP surfaces possess surface sensible heating;
- SLPSH: Only the sloping TP surface possesses surface sensible heating; and
- TOPSH: Only the top TP surface possesses surface sensible heating.

Then the differences between the three pairs, that is, ALLSH–NOSH, SLPSH–NOSH, and TOPSH–NOSH, can be considered: the impacts on the circulation of the TP due to all-surface sensible heating, sloping-surface sensible heating alone, and top-surface sensible heating alone. Their differences in horizontal wind and vertical motion at the lower model level $\sigma = 0.991$ are presented in Fig. 4. Coastlines are added into the figure only for reference and comparison. In the all-surface sensible heating case (Fig. 4a), surface air from the Arabian Sea, Indian subcontinent, BOB, Indochina peninsula, and the other neighborhood areas are converged into the TP area and ascend over the TP. The enhanced upward movement of more than -0.2 Pa s^{-1} is on its southern and eastern slopes where the release of latent heating further intensifies the ascent. The sloping-surface sensible heating produces similar circulations (Fig. 4b) as in the case with the surface sensible heating on all the TP surfaces (Fig. 4a) except over the platform: due to the absence of the in situ surface sensible heating, air descends over its top in association with radiation cooling. On the other hand, the mere top-surface sensible heating produces convergence flow only above the platform where the elevation is already higher than 3 km (Fig. 4c). There is no convergence at the lower elevations, and the main ascent appears over the eastern TP as a stationary Rossby wave response to the top-surface heating. The results shown above can be explained by using the right panels in Fig. 4. In the presence of surface sensible heating on the sloping surfaces (Figs. 4a,b), the heated air particles at the sloping surface penetrate the isentropic surfaces and slide upward. The air in the lower-elevation layers in the surrounding areas is therefore pulled into the plateau region, forming strong rising motion and even heavy rainfall over the TP. On the contrary, in the top-heating-only case (Fig. 4c), the platform heating can result in air convergence above the plateau and cannot pull air from below. This is because when an air particle is traveling in the lower layer and impinging on the TP, it has to stay at the same isentropic surface due to the absence of diabatic heating from the sloping lateral surface of the TP. Therefore, the air particle just goes around the TP at a rather horizontally located θ surface and no apparent ascent occurs. Thus there are no significant impacts on monsoon rainfall.

3) Sensitivity numerical experiments: Winter

Similar design is also applied to the perpetual January experiments, in which the solar angle is fixed on 15 January. In January the surface sensible heat flux on the TP is weak and negative in NCEP–NCAR reanalysis (Fig. 1a), as well as in the GOALS model. To highlight the effects of the TP's surface cooling on circulation, instead of diagnosing the model outputs, a unified negative surface sensible heat flux of (-30 W m^{-2}) is imposed on the relevant TP surfaces in the experiments ALLSH, SLPSH, and TOPSH. By following the same procedures as in the perpetual July experiments, the corresponding results at the $\sigma = 0.991$ surface for such perpetual January experiments are obtained and shown in Figs. 4d–f. When all the TP surfaces have a negative sensible heat flux (ALLSH), an anticyclone circulation appears to the northwest and a cyclone circulation ap-

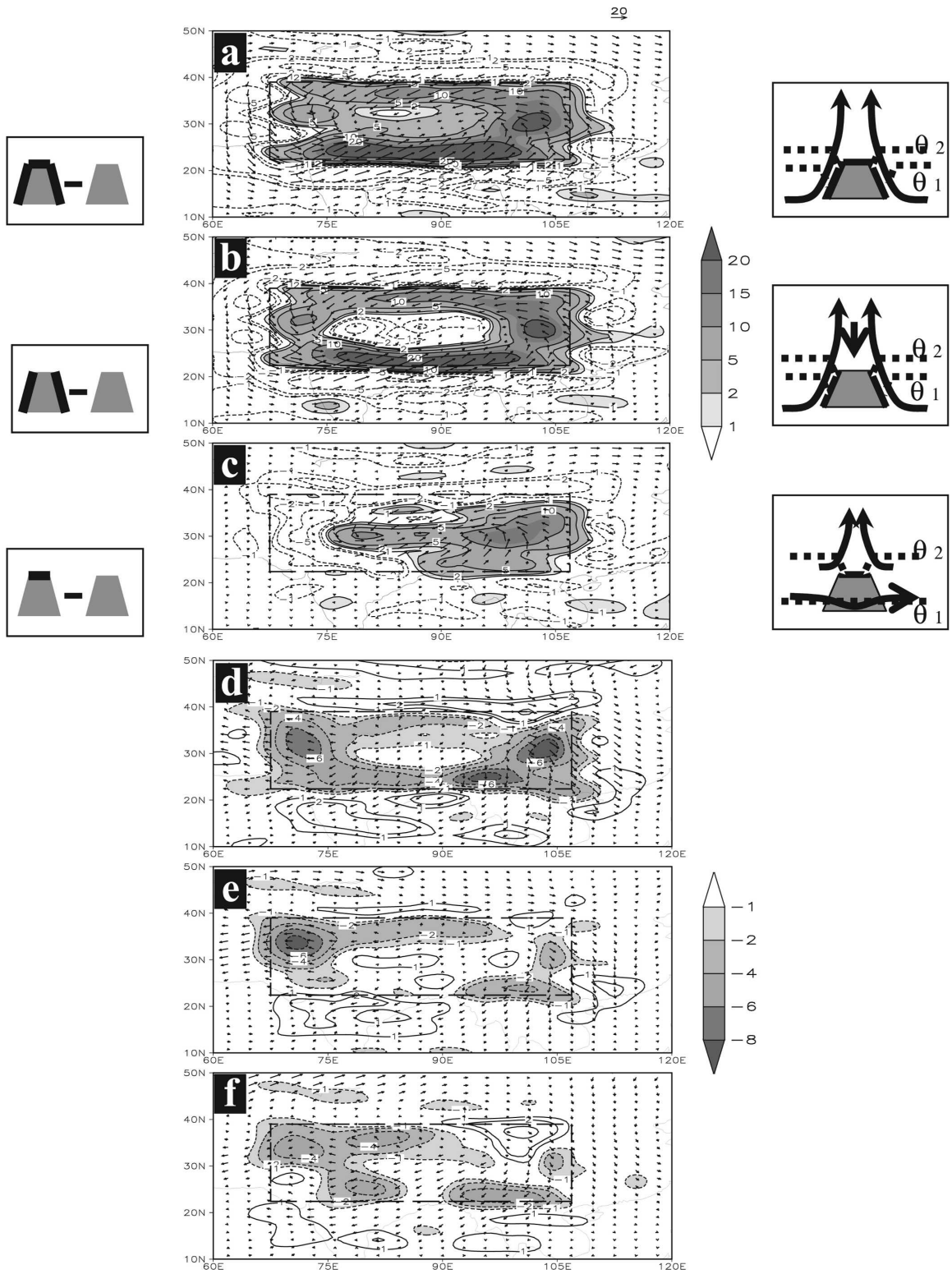

FIG. 4. Distributions of difference wind (vectors; m s^{-1}) and vertical velocity ($-\omega$; shading; 10^{-2} Pa s^{-1}) at the $\sigma = 0.991$ surface from the perpetual July experiments (a) ALLSH–NOSH, (b) SLPSH–NOSH, and (c) TOPSH–NOSH and from the perpetual January experiments (d) ALLSH–NOSH, (e) SLPSH–NOSH, and (f) TOPSH–NOSH. The rectangle in (a)–(f) indicates the mountain domain. Left panels indicate the experiment designs, and right panels indicate mechanism interpretations. See text for details.

pears to the northeast of the TP in the difference flow field between ALLSH and the experiment without surface heating (NOSH) (Fig. 4d). Easterly difference flow then slips down the western slope of the TP, while westerly difference flow slips down its eastern slope, and the surface air on the TP is diverged toward the surroundings. The difference in the wind field and vertical motion on the $\sigma = 0.991$ surface is shown in Fig. 4e for the difference between the experiment in which the negative sensible heat flux is only imposed on the sloping lateral surface (SLPSH) and the experiment NOSH. The down-sliding flow on both the western and eastern sloping surfaces and the diverging flow in the neighborhood of the TP are similar to those presented in Fig. 4d, though the intensity becomes weaker. When the negative sensible heat flux is only imposed on the top surface (TOPSH), the corresponding difference fields between TOPSH and NOSH are shown in Fig. 4f. In this case, the outward flow to the east and west of the TP is much weaker. Results from the perpetual January experiments then imply that the surface cooling of the TP on its sloping lateral boundary in wintertime also plays an important role in diverging cold air to the surrounding areas. We can now come to an important conclusion that the air pump over the TP can regulate the A–A monsoon only because the cooling/heating of its sloping surface can diverge/converge the air in the lower layer into/from the surrounding areas. In other words, the air pump of the TP as defined by Wu et al. (1997a, 2004) can be expressed as TP-SHAP. Comparing Figs. 4d–f with Figs. 4a–c, we see that in January the diverging impact of the TP-SHAP on the surrounding circulation is not as strong as its converging impact in summertime. This is because in summer the converging impact of the TP-SHAP is intensified by the condensation heating over the TP. In other words, there exists positive feedback between the small-scale convection over the TP and the large-scale convergent spiral circulation in the lower troposphere in the surroundings, manifesting as a kind of conditional instability of the second kind (CISK; Charney and Eliassen 1964). Besides, in the following we will see that in the winter season the mechanical forcing of the TP is more important.

The above finding is of practical significance both in numerical model development and field experiment design. For years we have tried to get observational data over the TP. In 1979 and 1998, China organized two large-scale field experiments in association with the FGGE and GEWEX programs (Zhang et al. 1988; Zhou et al. 2000), respectively. The main observation networks for the two experiments cover much of the TP platform. Although many important features concerning the thermal state and the energy balance on the TP have been revealed, not much is related to the circulations and monsoon. Results from this study show that in order to better understand the impacts of the energy state over the TP on the water cycle associated with the A–A monsoon, we need to pay more attention to the energy state on the sloping surface of the TP, particularly on its southern and eastern slopes.

b. TP Forcing and seasonal variation of the general circulation over Asia

1) TP-SHAP AND THE ABRUPT SEASONAL TRANSITION OF THE MONSOON CIRCULATION

The operation of the TP-SHAP has profound impacts on the Asian climate. It anchors the earliest Asian monsoon onset venue over the region from the eastern BOB to the western part of the Indochina peninsula (Wu and Zhang 1998; Liang et al. 2005). Its forcing also contributes to the abrupt seasonal transition of the nearby circulation as first reported by Yeh et al. (1959). To demonstrate this, the low-resolution version R15L9 of the GOALS-SAMIL model is employed to initiate a set of sensitivity experiments. In the first experiment, for the calculation of radiation the cloud distributions are prescribed by using satellite remote sensing data. The observed distributions of sea surface temperature and sea ice from 1979 to 1988, which were set for the AMIP experiments, are introduced as the prescribed lower-boundary conditions to integrate the model for 10 yr. This is defined as the CON run. The second experiment is the same as CON except that the sensible heating over the Tibetan Plateau region where the elevation is higher than 3 km is not allowed to heat the atmosphere aloft. This is achieved by switching off the sensible heating term in the thermal dynamic equation at the grid points over the plateau region. This experiment is then defined as the NSH run. Since the cloud amounts for the calculation of radiation are prescribed, there is no cloud–radiation feedback in the model, and since the ground surface temperature in the model is calculated based on the thermal equilibrium assumption, the energy budgets at the ground surface in the two experiments are kept unchanged. Therefore, the differences between these two experiments can be considered as resulting purely from the sensible heating over the plateau.

Figure 5 shows the mean seasonal evolution of the simulated zonal wind component and the ridgeline of the subtropical anticyclone as identified by the $u = 0$ contour at 300 hPa and along 90°E. In the CON run, the westerly jet is strong in winter with its center located near 35°N but is weak in summer with its center north of 40°N. The ridgeline of the subtropical anticyclone is

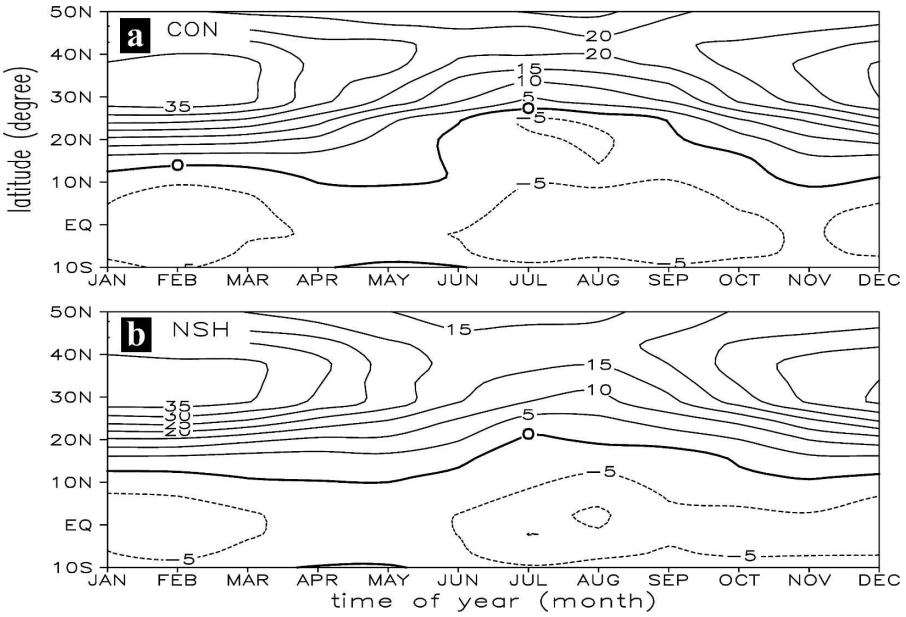

FIG. 5. Seasonal evolution of the zonal wind component ($m\ s^{-1}$) and the ridgeline of the subtropical anticyclone (represented by $u = 0$) along 90°E at 300 hPa in the model experiment (a) CON and (b) NSH.

located near 12°N in the winter months from November to May and near 30°N in the summer months from June to October. An abrupt northward jump of the ridgeline from its winter location to its summer location occurs near the end of May. In one pentad it jumps north by more than 15°, mimicking the abrupt seasonal transition reported by Yeh et al. (1959). However, in the NSH run, such an abrupt seasonal transition disappears, and the northward migration of the ridgeline of the subtropical anticyclone becomes rather smooth. This is because in spring, as the surface sensible heating over the TP increases, the anticyclone in the upper troposphere intensifies gradually. Soon after the Asian monsoon onset occurs over the BOB and the Southern China Sea (SCS), due to the large latent heat release associated with monsoon rainfall, the strong northerly winds over East Asia and the strong south Asian high over the south of the TP are forced (Wu et al. 1999, Wu and Liu 2000; Liu et al. 1999, 2001). The south Asian high is so strong that the wintertime westerly winds to the south are reversed to easterly winds and the westerlies to the north are intensified. The northward "jump" of the westerly winds and of the subtropical anticyclone is then completed. In the absence of the elevated sensible heating over the TP, the Asian monsoon and the summertime south Asian high are rather weak, and no apparent abrupt changes in circulation are observed.

2) TP FORCING AND THE ASSOCIATED WINTER AND SUMMER CIRCULATION PATTERNS

The seasonal evolution of the thermal state averaged over the TP area can be calculated by employing the monthly mean NCEP–NCAR reanalysis. Since the surface elevation varies greatly in different parts of the area, and the atmospheric diffusive heating associated with surface sensible heat flux vanishes rapidly with increasing height, the σ-vertical coordinate is adopted for plotting different heating profiles averaged over the area in different seasons. As shown in Fig. 6, radiation always cools the atmosphere over the TP, with a maximum radiation cooling rate of 2–3 K day^{-1} at $\sigma = 0.85$. Condensation heating due to latent heat release is significant during the summer. It warms the atmosphere by more than 3 K day^{-1} over most of the troposphere, with a maximum of more than 5 K day^{-1} at $\sigma \approx 0.95$. Condensation heating is also important in spring, which compensates for the radiation cooling in the free atmosphere. It becomes much weaker in autumn and winter. The most striking feature appears in the vertical profiles of sensible heating. First, it is a lower-layer heating that approaches zero at $\sigma = 0.85$ in January and at $\sigma = 0.75$ in April before the monsoon onset. Second, the surface heating is negative in January (~ -2 K day^{-1}) but strongly positive in July (~ 12 K day^{-1}), possessing the largest seasonal cycle and accounting for the diverging effect in winter and converg-

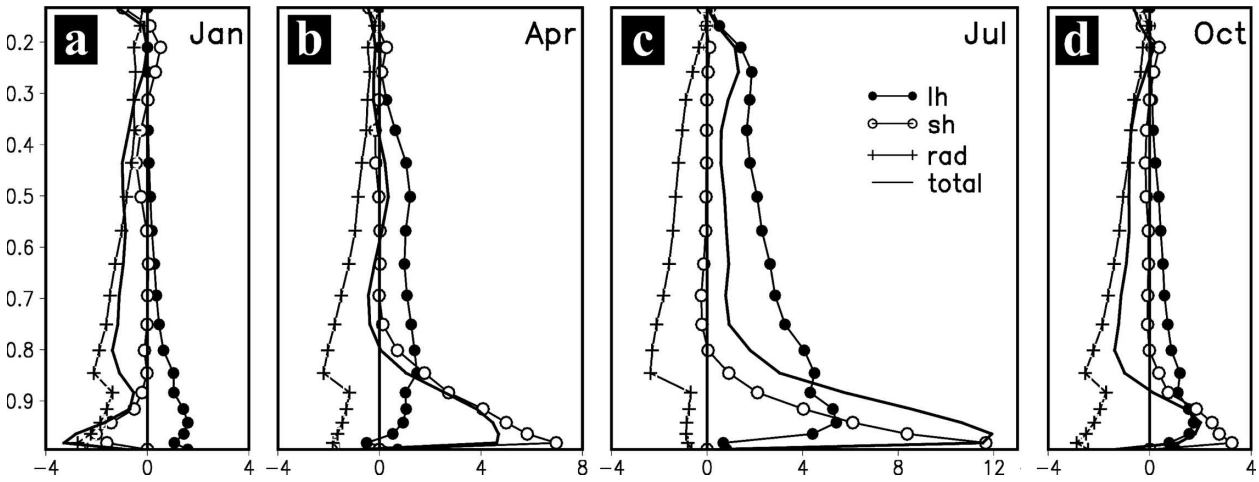

FIG. 6. Vertical heating profiles in difference seasons over the Tibetan Plateau area (27.5°–37.5°N, 80°–100°E) from NCEP–NCAR for 1980–97: (a) January, (b) April, (c) July, and (d) October. lh: latent heating; sh: sensible heating; rad: radiation cooling; and total: total heating. Unit is K day^{-1};

ing effect in summer of the aforementioned TP-SHAP on the surrounding atmosphere. Because the near-surface sensible heating is very strong, the shape of the total heating profile follows that of sensible heating quite well in all seasons. At the surface the total surface heating flux is downward in winter but strongly upward in summer (see also Fig. 1a). The whole total heating profile is negative in January but positive in July. It then demonstrates that the whole atmospheric column over the TP is a heat sink in winter and a heat source in summer.

Because Fig. 6 is based on the NCEP–NCAR reanalysis, and because reanalysis products are model dependent, caution is needed when these results are employed for research. Table 1 shows the surface sensible heat flux and the column-integrated total heating averaged over the TP area in different months and calculated for the period 1980 to 1999 from different sources. The nature of model dependence of the reanalysis data can be seen clearly in Table 1. The surface sensible heat flux over the TP calculated from NCEP–NCAR and NCEPII are quite similar, possessing negative flux in January and similar annual cycles, although the fluxes in April and July obtained from NCEPII are about 8 W m^{-2} larger than from NCEP–NCAR and closer to observations (Duan and Wu 2005). However, these results are different from their counterparts calculated from the 40-yr ECMWF Re-Analysis (ERA-40). In ERA-40, the flux in January is no longer negative, and its maximum appears in spring rather than summer. For the volume-integrated total heating the two datasets, NCEP–NCAR and ERA-40, possess similar seasonal changes, but the latter always exceeds the former by more than 30 W m^{-2}, with the minimum of 34.28 W m^{-2} in July and the maximum of 82.38 W m^{-2} in April. Therefore, although the general features concerning the TP heating (Fig. 6) are in agreement with other reanalysis and in situ observations (Duan and Wu 2005), the magnitudes presented here are different and the results obtained below should be considered qualitative in nature.

The seasonal variation of the thermal state over the TP has profound influence on the general circulation of the atmosphere. Figures 7a,b depicts the winter and summer mean distributions of potential temperatures at 850 hPa and the stream field of the wind deviations from their corresponding zonal means. The distributions of the stream field presented in this figure are similar to the corresponding stream fields of Wu et al. (2005, their Figs. 5a,d), which are composed of the wind difference between two numerical experiments with and without the topography over the Eurasian conti-

TABLE 1. Surface sensible heat flux and the column-integrated total heating averaged over the TP area (27.5°–37.5°N, 80°–100°E) in different months and calculated for the period 1980 to 1999 from different data sources (W s^{-2}).

	Surface sensible heat flux			Column-integrated heating	
Month	NCEP–NCAR	NCEPII	ERA-40	NCEP–NCAR	ERA-40
Jan	−19.48	−13.15	8.62	−66.50	−25.85
Apr	44.33	52.93	48.95	26.71	109.09
Jul	56.08	63.24	35.97	141.08	175.36
Oct	13.25	13.32	29.55	−34.72	9.81

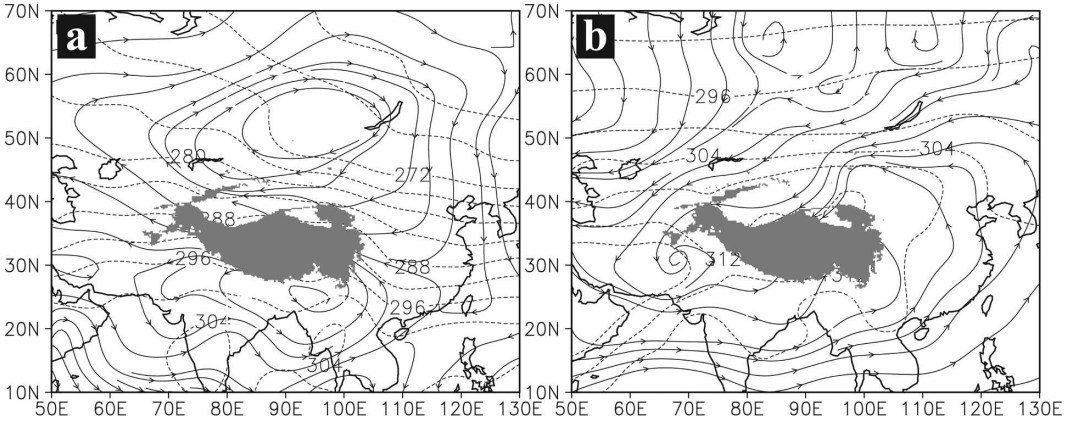

FIG. 7. Distributions at 850 hPa of the potential temperature (K) and of the stream fields composed of wind deviations from the corresponding zonal means based on the NCEP–NCAR reanalysis for 1968–97. (a) Winter average between December and February; (b) Summer average between June and August. Shading indicates where the elevation exceeds 3000 m.

nent. Therefore, the features of Fig. 7 could be considered to be largely due to the impacts of the topography on circulation. In winter months, the topography retards the impinging midlatitude westerly winds and deflects the flow from zonal to circumcolumnar (Fig. 7a). The deviation streamlines depict an asymmetric dipole shape with an anticyclone to the north of the TP and a cyclone to the south. The streamlines then converge over eastern China and go into its "eastern pole" but come out of its "western pole" and diverge over middle Asia. The anticyclonic deviation circulation gyre in high latitudes advects warm air to the north on the west of the gyre but cold air to the south on its east. As a result, the isotherms at high latitudes in Asia tilt from northwest to southeast, and the temperature at 130°E is colder than that at 50°E by 10 K at 40°N and 14 K at 50°N. On the other hand, the cyclonic deviation circulation gyre in low latitudes advects dry air southward to the south Asia subcontinent but moist air northward to the Indochina peninsula and south China. As a result, a prolonged dry season in south Asia and persistent rainy season in Southeast Asia and south China are observed before the Asian monsoon onset. In the summer months, the strong TP heating excites a huge cyclonic deviation circulation over East Asia, and the strong pulling of the TP-SHAP makes the surrounding flows converge into the TP area. Therefore, the summer pattern of the deviation stream field at 850 hPa resembles a huge "cyclonic spiral" and the TP-SHAP looks like a spiral pump. In fact, the summer TP is an important genesis location of vortices that can propagate eastward and result in torrential rain along the Yangtze River (Tao 1980).

3. Influence of the TP-SHAP on Asian climate

a. Persistent rainfall in early spring over south China

Besides the well-known Asian monsoon, another less-known unique feature of Asian rainfall is the occurrence of PRES over southern China. From late February to early May (pentad 12–26) before the onset of the Asian monsoon, persistent rains occur over a large area south of the Yangtze River (Fig. 8). Southern China is an important agricultural area with abundant rice fields. Heavy PRES is often accompanied by cold temperatures, which can rot rice seedlings and cause agricultural catastrophe. However, the formation mechanism is still unclear. Tian and Yasunari (1998) noticed that the PRES occurs because there is ample water vapor transported into the region by southerly winds from the SCS. They then proposed a mechanism of time lag in the spring warming between land and sea to explain the formation of the PRES. In early spring the Indochina peninsula west of the SCS warms more rapidly than the western North Pacific to the east of SCS. The surface pressure gradient is then oriented eastward across the SCS, forming southerlies and contributing to the occurrence of PRES. However, a recent study by Wan and Wu (2007; Fig. 6) shows that such a heating time-lag mechanism also exists between Mexico and the western North Atlantic in the same period, but there are no PRES in North America. It seems that the time-lag heating mechanism could be a necessary but not a sufficient condition for the formation of PRES.

As demonstrated in Fig. 7a, before the monsoon onset the TP can generate a dipole-type circulation pattern. The deflected flow brings cold, air from the north

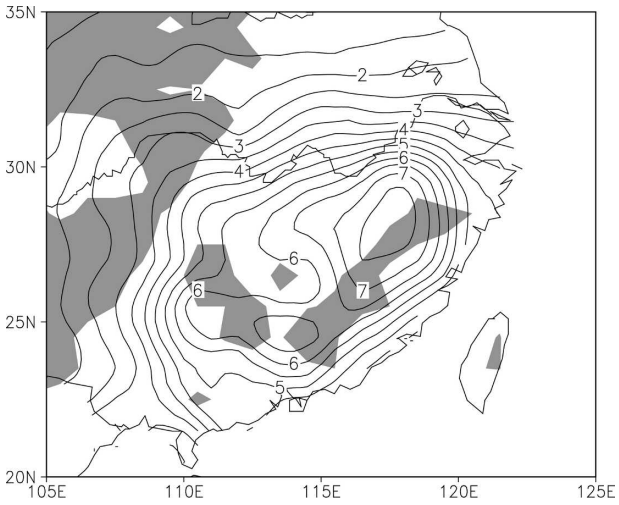

FIG. 8. Distribution of mean rainfall (mm day^{-1}) the period of PRES (pentad 12–26) over China averaged between 1951 and 2000. Shading indicates where the elevation exceeds 600 m; from Wan and Wu (2007).

and moist, air from the south, which then converge over eastern China. This may contribute to the formation of PRES. To verify this hypothesis, a series of numerical experiments were conducted by Wan and Wu (2007; Fig. 12). For our purpose, the R42L9 GOALS-SAMIL is employed again. Results of its long-term integration show the ability of the model in simulating the observed mean climate. Figures 9a,b display the distributions of the simulated wind vector at 850 hPa and rainfall in April. Strong southwesterly winds on the southeastern flank of the TP and strong northwesterly winds to the far northeast agree well with observations, reflecting the deflection impacts of the TP on the basic flows as shown in Fig. 7a. The general features of PRES as shown in Fig. 8 are also well captured (Fig. 9b). There is an obvious rain area to the south of the Yangtze River, with a maximum of about 8 mm day^{-1}, consistent with observations (Fig. 8).

To focus on physical mechanisms, perpetual April integrations are designed in the following experiments. The solar angle is set to 10 April. Each experiment is integrated for 36 months, and the results from the last 30 months are retrieved for the following diagnosis. Experiments start with a case of "no mountains in Eurasia" in which the Eurasian continent is undercut and leveled to 0 km while the topography in other continents is kept unchanged. The other experiments are the same as the first except the Eurasian topography has increasing heights at an interval of 1 km. Figure 10 shows the wind vector at 850 hPa and rainfall in the experiments when the elevation of the TP is leveled at 0, 2, 4, and 6 km, respectively.

In the "no TP" experiment, the westerly jet in Eurasia does not split, and a zonal-oriented subtropical anticyclone belt dominates in the middle–low latitudes (Fig. 10a). Significant rainfall appears only in the southwest of the Indochina peninsula, in association with the easterly perturbation forced by land–sea thermal contrast (Fig. 10b). After the elevation of the TP reaches 2 km, the westerly jet starts to split into its northern and southern branches (Fig. 10c). They meet downstream of the TP, forming a strong Asian jet. The belt of subtropical anticyclone breaks and a prominent anticyclonic center appears over the western Pacific. Therefore the distribution of rainfall takes the shape of PRES (Fig. 10d). In the 4-km TP experiment, the split westerly jets on both north and south sides of the TP are strengthened, the circulation pattern (Fig. 10e) is already close to the simulation counterpart as shown in Fig. 9a, and the PRES appears (Fig. 10f). In the 6-km TP experiment, although the basic circulation pattern does not change very much, the two split westerly jets are much stronger (Fig. 10g), and the winter time TP Dipole circulation also becomes stronger compared to CON in which the seasonal variation is included (Fig. 9a). As a result, the PRES is weakened, and the main rainfall center moves to the eastern TP (Fig. 10h), where the convergent entrance pole of the TP dipole in the wintertime deviation streamline pattern is located.

The above experiments prove that PRES is formed mainly due to the deflecting effects of the TP. When the deflected flow—cold air from the north and warm, moist air from the south—meet downstream of the TP, PRES is formed. The experiments further demonstrate that the intensity and location of the PRES are to some extent influenced by the elevation of the TP.

b. Continental-scale heating, Tibetan Plateau heating, and East Asian climate

The atmospheric thermal response to diabatic heating is to generate a cyclonic circulation near the surface and an anticyclonic circulation in the upper layer, with a rising in the east and a sinking in the west (Gill 1980; Hoskins 1991; Wu and Liu 2000). Wu and Liu (2003) and Liu et al. (2004) found that in the summer months in the subtropics, the dominant heating over each continent and its adjacent oceans are organized in the following order from west to east: longwave radiation cooling (LO) over the western offshore region; surface sensible heating (SE) over the west; condensation heating (CO) over the east; and double-dominant heating (D) over the eastern offshore region. In association with such a LOSECOD quadruplet heating, a cyclonic circulation at the surface and an anticyclonic circulation in the upper troposphere are forced over land, whereas

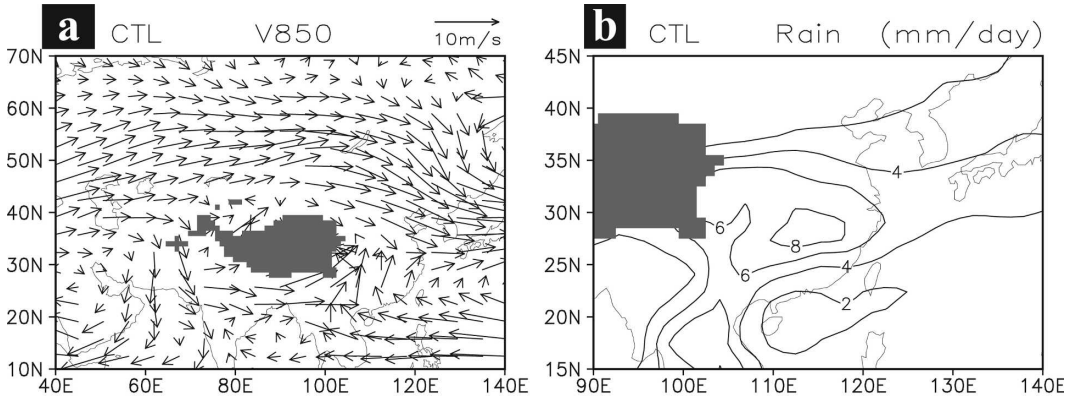

FIG. 9. Distributions of (a) wind vectors (m s^{-1}) at 850 hPa and (b) rainfall (mm day^{-1}) in spring (March and April means) averaged over 10 yr as simulated in the model GOALS-SAMIL. The shaded areas are where elevation exceeds 2500 m; based on Wan and Wu (2007).

a surface anticyclonic circulation and upper-tropospheric cyclonic circulation are forced over the ocean. Under the continental-scale heating, ascending motion and a moist climate appear over the eastern continent, whereas descending motion and dry climate prevail over its west.

As shown in Fig. 6c, the TP is a strong heat source in summer months with the strongest heating of about 12 K day^{-1} near the surface. Such a forcing should produce a shallow cyclonic circulation near the surface and an anticyclonic circulation over the deep layers aloft, with a rising in the east and a sinking in the west (Duan and Wu 2005). This is observed in the summer not only over the TP but also over the Iran plateau (Fig. 11). The meridional wind cross section (Fig. 11a) demonstrates that over each mountain there exist a shallow cyclonic circulation near the surface and an anticyclonic circulation in the deep upper layers. The cross section of vertical motion (Fig. 11b) shows that over each mountain range, rising air predominates over the central and eastern parts, whereas sinking is observed over the west. It is important to note that the rising motion over East Asia excited by the continental heating and the rising excited by the local TP heating link up into a single stretch (Fig. 11b) and become very strong (~ -0.1 Pa s^{-1}). Conversely, over middle Asia, the descending motions forced by both continental-scale heating and topography heating are in phase. The water cycle in this region is suppressed, and the local climate becomes rather dry.

The above diagnosis implies that because the TP and Iran plateau are located in the middle and eastern parts of the Eurasian continent, the water cycle over East Asia associated with the Asian monsoon is intensified. To prove this reasoning, three numerical experiments were designed by using the GOALS-SAMIL. This time an idealized land distribution mimicking the distribution of the Eurasian and Africa continents and the India and Indochina subcontinents (as marked in Fig. 12) is added to the aquaplanet. Each experiment is integrated for 10 yr, and the results averaged from the last 8 yr are retrieved for diagnosis. The first experiment does not have any mountains. In the second experiment an idealized ellipsoidal topography with a maximum height of 5 km is embedded in the land area centered at 32.5°N, 87.5°E to mimic the TP. In the third experiment, this idealized ellipsoidal topography is moved westward to 32.5°N, 60°E, to just north of the "Arabian Sea." The results presented in Fig. 12 show that in the absence of topography (Fig. 12a), the Eurasian continent in the summer months forces a huge continental-scale cyclone at 850 hPa with southerly flow of 4 m s^{-1} off its eastern coast and northerly flow of 6 m s^{-1} off its western coast. A weak East Asian monsoon of 8 mm day^{-1} is forced over its southeastern corner, with the rainband tilting from southwest to northeast. The northeast tilt of the summer rainband in the absence of the TP contributes to the observed east–west contrast between monsoonal climate in East Asia and dryness in the Sahara. Based on a highly simplified experiment with idealized coastline, Xie and Saiki (1999) discussed this tilted rainband due to the northward moisture advection on the east coast and southward advection on the west coast of a major continent. Chou et al. (2001) used an intermediate-complexity atmospheric model coupled with a simple land surface model and a mixed layer ocean model to investigate the processes involved in an idealized monsoon occurring on a single rectangular continent. They found that the inclusion of an upward ocean heat transport favors continental convection. The monsoon circulation then produces a moisture transport from the ocean regions that allows sub-

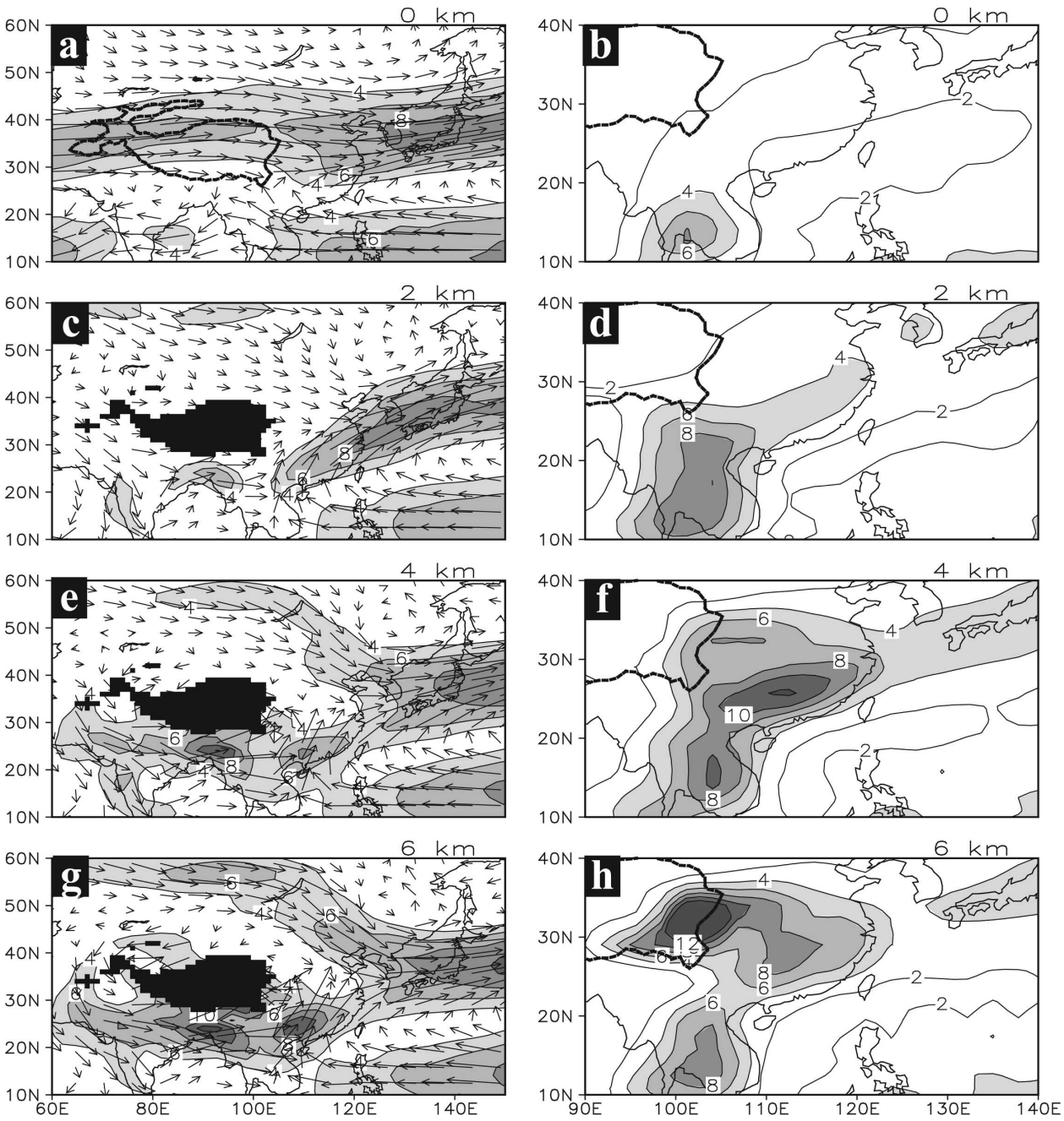

FIG. 10. Distributions of (left) wind vectors and isotachs at 850 hPa (m s^{-1}; shading indicates >4, 6, 8 m s^{-1}) and (right) rain (mm day^{-1}) in the perpetual spring sensitivity experiments with different TP elevations and averaged over 30 months. The black shading in the left panels and bold solid curve in the right panels are the main part of TP. The TP maximum elevation is 0 km in (a) and (b), 2 km in (c) and (d), 4 km in (e) and (f), and 6 km in (g) and (h); from Wan and Wu (2007).

stantial progression of convection into the subtropics over the eastern portion of the continent. Chou et al. consider this east–west asymmetry to be partly due to the interactive Rodwell–Hoskins mechanism (Rodwell and Hoskins 1996).

When the topography is centered near 90°E (Fig. 12b), two cyclonic systems in the 850-hPa wind field can be clearly identified. One is the continental-scale cyclone that is similar to the one presented in Fig. 12a, with the intensity of the northerly flow of 6 m s^{-1} off its western coast almost unchanged. The other is just encircling the TP with the northerly flow on its western

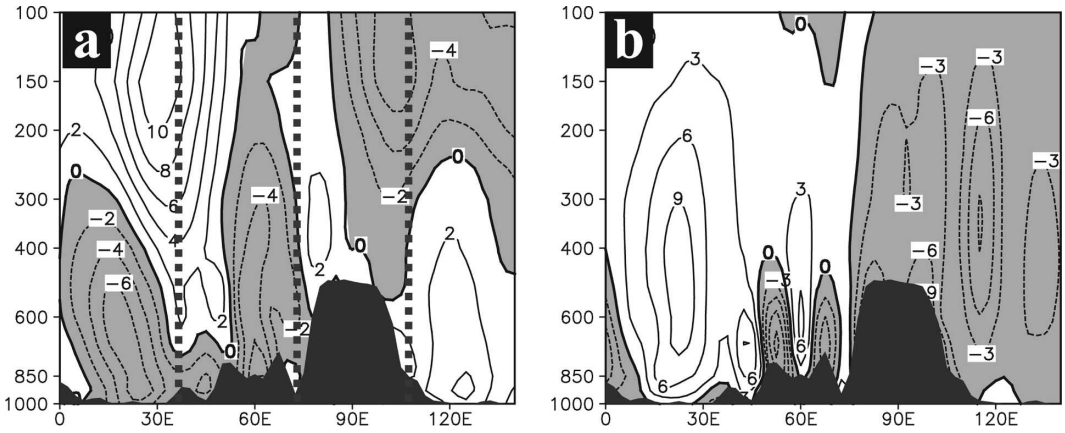

FIG. 11. Longitude-pressure cross sections (a) along 32.5°N of the July mean meridional wind ($m\ s^{-1}$) and (b) vertical velocity (in p units of 10^{-2} Pa s^{-1}) from NCEP–NCAR for 1981–99; from Duan and Wu (2005).

flank and the southerly flow on its eastern flank that overlaps with the southerly flow forced by the continental heating and is enhanced to 10 m s^{-1}. The northerly flow on the west is quite strong (greater than 8 m s^{-1}). It advects cold and dry air from the Asian inland area and contributes to the formation of the desert climate in the middle of Asia. He et al. (1987) showed that the dry descent over middle Asia after the onset of the Indian monsoon is induced by the upper-layer divergence over the monsoon rainfall region (their Fig. 15c). Yanai et al. (1992) described this dry descent over the Iran–Afghanistan region in more detail. Rodwell and Hoskins (1996) interpret the formation of the desert climate in middle Asia in terms of the westward Rossby wave forcing that is triggered by the latent heating of the Asian monsoon and interacts with the westerly flow over middle Asia. Here we show that the TP forcing can also contribute to the formation of the desert climate in middle Asia. However, when the topography is moved westward to 60°E (Fig. 12c), while the cyclonic circulation forced by continental heating does not change very much compared with its counterpart in the no-topography experiment as shown in Fig. 12a, the cyclonic circulation that encircles the TP in Fig. 12b has moved westward. The southerly flow associated with the continental heating is about 8 m s^{-1} and that associated with the topography forcing also about 8 m s^{-1}. However, these two southerly bands are quite separated, and the strong East Asia monsoon rainbelt that exists in the previous experiment (Fig. 12b) now splits into two belts, one over the southeastern corner of the continent that is rather similar to its counterpart in the no-topography case (Fig. 12a) and the other on the eastern flank of the TP. On the other hand, the northerly flow on the western flank of the TP overlaps with that forced by continental heating; thus, the area with northerly flow stronger than -2 m s^{-1} is expanded. We can then reach the conclusion that the strong East Asian monsoon and the associated water cycle occur because the continental forcing and TP forcing act to enhance the rising motion and water cycle over the East Asian area.

4. Summary and outlook

The huge TP is one of the earth's most impressive topographical features. Its mechanical forcing and unique elevated thermal forcing have a large influence on global as well as regional climate. The TP is a weak heat sink in winter and a strong heat source in summer. Mainly driven by the sensible heating at its sloping surfaces, the wintertime cold air particles above the TP descend along the cooling sloping surfaces, being pumped into the surrounding areas, whereas the summertime warm ascending air particles above the TP pull the air from below, and the lower tropospheric air from the surrounding areas are converged toward the TP area and climb up the heating sloping surfaces. It is shown that such a TP air pump is mainly driven by the surface sensible heating on TP, particularly on its sloping lateral surfaces. It is defined as the sensible heat driving air pump of the Tibetan Plateau. It contributes significantly to the seasonal reversal of the airflows in the Asian–Australian monsoon areas. The impact of the pulling on the atmospheric circulation in summer is stronger than its expelling impact in winter because in the summer months there is CISK-like positive feedback between the small-scale convection over the TP and the large-scale convergent spiral of the lower-tropospheric circulation in the surrounding area. The absence of the sensible heating on the sloping lateral surface of the TP can shut off such a CISK mechanism and significantly weakens the TP air pump.

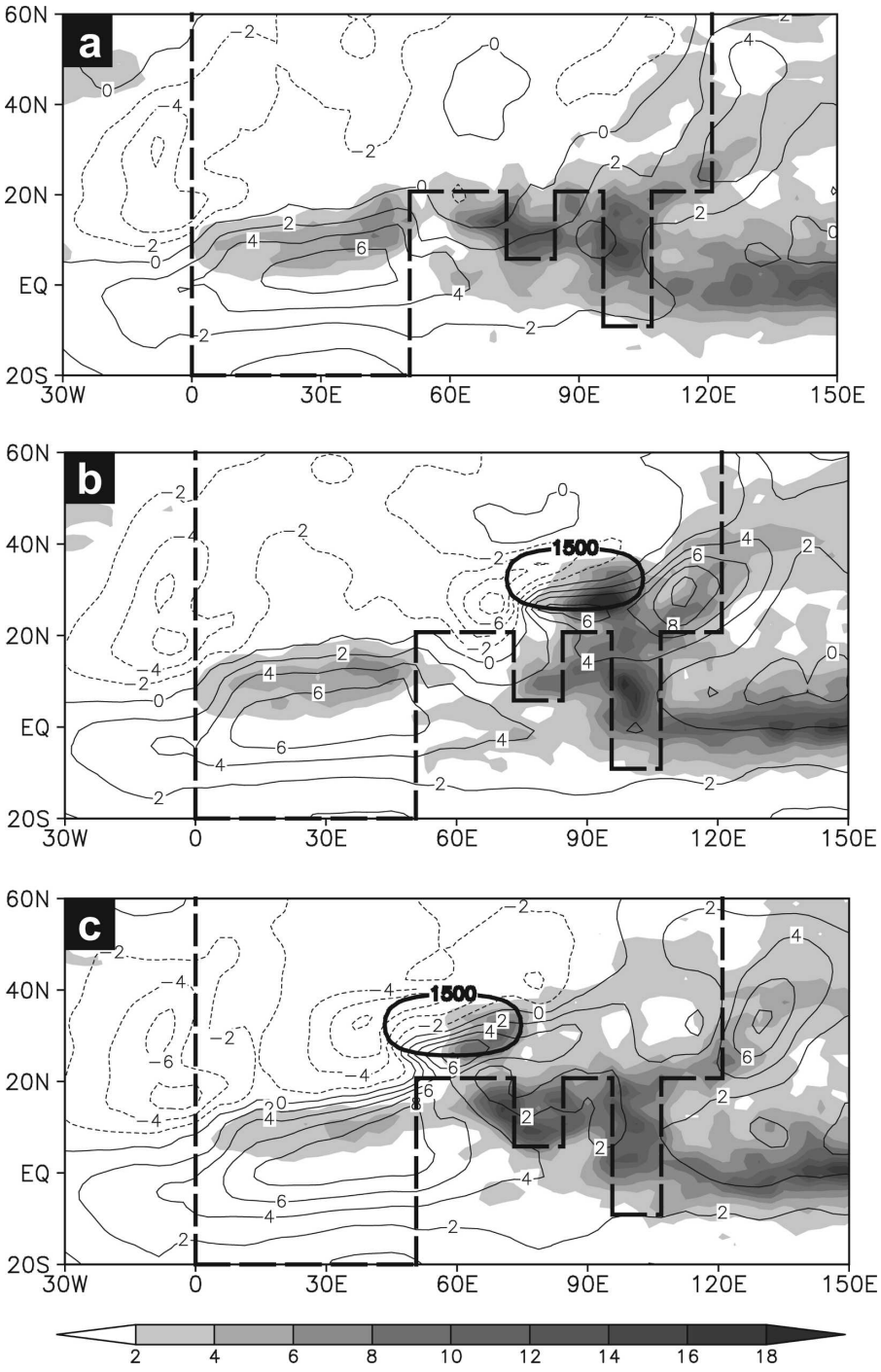

FIG. 12. Distributions of the 8-yr July mean meridional wind at 850 hPa (contours; interval 2 m s^{-1}) and rainfall (shading; mm day^{-1}) in the idealized experiment (a) no mountain; (b) mountain centered at (32.5°N, 87.5°E); and (c) mountain centered at (32.5°N, 60.0°E). The heavy dashed line denotes the idealized coastlines; and the heavy ellipse in (b) and (c) indicates the location of orography at the elevation of 1500 m.

In winter as a large obstacle, the TP retards the westerly jet flow and deflects it into northern and southern branches. The deviation streamflow then appears as an asymmetric dipole with the convergent entrance on its eastern flank and the divergent outgoing on its western flank. The huge anticyclonic-deflected flow in the north has an important impact on atmospheric temperature distributions due to its horizontal advection, making

East Asia much colder than middle Asia. Its cyclonic-deflected flow in the south has an important impact on the dry climate in south Asia and the moist climate in Southeast Asia and south China. In late winter and early spring over south China, the southward-moving cold and dry air that flows along the northern anticyclonic circulation of the TP dipole meets with the northward-moving warm and moist air that flows along the southern cyclonic circulation of the TP dipole. Persistent rainfall in early spring (PRES) therefore occurs over south China till the Asian monsoon onset. In late spring, the TP heating also contributes to the establishment and intensification of the south Asian high and the abrupt seasonal transition of the surrounding circulations. In summer, the TP heating produces a large-scale cyclonic circulation in the lower troposphere. Such a forcing in conjunction with the TP air pump causes the deviation stream field to resemble a cyclonic spiral, converging toward and rising over the TP.

The TP together with the Iran plateau are located in the central and eastern parts of the Eurasian continent. The meridional and vertical motions generated by the Eurasian continental-scale heating are in phase with those generated by the TP local-scale heating over Asia. Southerly flow rises over East Asia and the northerly flow sinks over middle Asia and therefore becomes very strong. The Asian monsoon climate and the middle Asia dry climate in summer are intensified by the TP heating.

The influence of the TP on the Asian monsoon onset is another important issue. This will be reported in a separate paper. The monsoon system is a complex system (Webster et al. 1998). Despite the great research efforts made on this issue, many aspects are still unclear. Unresolved questions include how radiation processes affect the thermal state of the TP, how the aerosol–cloud–radiation monsoon circulation feedback occurs in the TP area, how the air–sea exchange processes interact with such a feedback, and how the TP air pump in conjunction with the thermal state over the Indian Ocean and Australia affect the Asia–Australia monsoon. These are topics that need to be studied with the cooperation between GEWEX and other programs under the WCRP umbrella.

Acknowledgments. This study is jointly supported by the 973 program 2004CB418300 and 2006CB403607, CAS International Partnership Creative Group "The Climate System Model Development and Application Studies," and by the National Natural Science Foundation of China 40475027, 40405016, 40575028, 40575044, and 40221503. The authors are grateful to the three anonymous reviewers and Dr. Shangping Xie whose comments helped to improve the manuscript and to Dr. Justin Ventham from the University of Hawaii and Ms. Carolyn Ehn from the International GEWEX Project Office (IGPO) for their kind help in improving the English. We thank Dr. Rick Lawford for his great efforts in organizing this special issue.

REFERENCES

Annamalai, H., J. M. Slingo, K. R. Sperber, and K. Hodges, 1999: The mean evolution and variability of the Asian summer monsoon: Comparison of ECMWF and NCEP–NCAR reanalyses. *Mon. Wea. Rev.,* **127,** 1157–1186.

Bolin, B., 1950: On the influence of the earth's orography on the westerlies. *Tellus,* **2,** 184–195.

Charney, J. G., and A. Eliassen, 1949: A numerical method for predicting in the perturbation of the middle latitude westerlies. *Tellus,* **1,** 38–54.

——, and ——, 1964: On the growth of the hurricane depression. *J. Atmos. Sci.,* **21,** 68–75.

Chou, C., J. D. Neelin, and H. Su, 2001: Ocean–atmosphere–land feedbacks in an idealized monsoon. *Quart. J. Roy. Meteor. Soc.,* **127,** 1869–1891.

Duan, A. M., 2003: The influence of thermal and mechanical forcing of Tibetan Plateau upon the climate patterns in East Asia. Ph.D. thesis, Institute of Atmospheric Physics, Chinese Academy of Sciences, 161 pp.

——, and G. X. Wu, 2005: Role of the Tibetan Plateau thermal forcing in the summer climate patterns over subtropical Asia. *Climate Dyn.,* **24,** 793–807.

Flohn, H., 1957: Large-scale aspects of the "summer monsoon" in South and East Asia. *J. Meteor. Soc. Japan,* **35,** 180–186.

——, 1968: Contributions to a meteorology of the Tibetan Highlands. Atmospheric Science Paper 130, Colorado State University, 120 pp.

Gill, A. E., 1980: Some simple solutions for heat-induced tropical circulation. *Quart. J. Roy. Meteor. Soc.,* **106,** 447–462.

He, H., J. W. McGinnis, Z. Song, and M. Yanai, 1987: Onset of the Asian summer monsoon in 1979 and the effect of the Tibetan Plateau. *Mon. Wea. Rev.,* **115,** 1966–1995.

Hoskins, B. J., 1991: Towards a PV-θ view of the general circulation. *Tellus,* **43AB,** 27–35.

Hung, C.-W., and M. Yanai, 2004: Factors contributing to the onset of the Australian summer monsoon. *Quart. J. Roy. Meteor. Soc.,* **130,** 739–761.

——, X. Liu, and M. Yanai, 2004: Symmetry and asymmetry of the Asian and Australian summer monsoons. *J. Climate,* **17,** 2413–2426.

Kalnay, E., and Coauthors, 1996: The NCEP/NCAR 40-Year Reanalysis Project. *Bull. Amer. Meteor. Soc.,* **77,** 437–471.

Kuo, H. L., and Y. F. Qian, 1982: Numerical simulation of the development of mean monsoonal circulation in July. *Mon. Wea. Rev.,* **110,** 1879–1897.

Li, C., and M. Yanai, 1996: The onset and interannual variability of the Asian summer monsoon in relation to land–sea thermal contrast. *J. Climate,* **9,** 358–375.

Li, G. P., T. Y. Duan, and Y. F. Gong, 2000: The bulk transfer coefficients and surface fluxes on the western Tibetan Plateau. *Chin. Sci. Bull.,* **45,** 1221–1226.

——, T. Duan, S. Haginoya, and L. Chen, 2001: Estimates of the bulk transfer coefficients and surface fluxes over the Tibetan Plateau using AWS data. *J. Meteor. Soc. Japan,* **79,** 625–635.

Liang, X. Y., Y. M. Liu, and G. X. Wu, 2005: Effect of Tibetan Plateau on the site of onset and intensity of the Asian summer monsoon. *Acta Meteor. Sin.,* **63,** 799–805.

Liou, K. N., and X. L. Zhou, 1987: *Atmospheric Radiation: Progress and Prospects, Proceedings of the Beijing International Radiation Symposium—Beijing, China, August 26–30, 1986.* Science Press and Amer. Meteor. Soc., 699 pp.

Liu, H., and G. X. Wu, 1997: Impacts of land surface on climate of July and onset of summer monsoon: A study with an AGCM plus SSiB. *Adv. Atmos. Sci.,* **14,** 289–308.

Liu, X., G. X. Wu, W. P. Li, and Y. M. Liu, 2001: Thermal adaptation of the large-scale circulation to the summer heating over the Tibetan Plateau (in Chinese). *Prog. Nat. Sci.,* **11,** 207–214.

——, W. P. Li, and G. X. Wu, 2002: Interannual variations of the diabatic heating over the Tibetan Plateau and the northern hemispheric circulation in summer. *Acta Meteor. Sin.,* **60,** 267–277.

Liu, Y. M., G. X. Wu, H. Liu, and P. Liu, 1999: Impacts of spatial differential heating on the formation and variation of the subtropical anticyclone, III. Condensation latent heating and South Asian high and the subtropical anticyclone over western Pacific. *Acta Meteor. Sin.,* **57,** 525–538.

——, ——, ——, and ——, 2001: Condensation heating of the Asian summer monsoon and the subtropical anticyclone in the Eastern Hemisphere. *Climate Dyn.,* **17,** 327–338.

——, ——, and R. C. Ren, 2004: Relationship between the subtropical anticyclone and diabatic heating. *J. Climate,* **17,** 682–698.

Luo, H., and M. Yanai, 1983: The large-scale circulation and heat sources over the Tibetan Plateau and surrounding areas during the early summer of 1979. Part I: Precipitation and kinematic analyses. *Mon. Wea. Rev.,* **111,** 922–944.

——, and ——, 1984: The large-scale circulation and heat sources over the Tibetan Plateau and surrounding areas during the early summer of 1979. Part II: Heat and moisture budgets. *Mon. Wea. Rev.,* **112,** 966–989.

Mao, J., G. Wu, and Y. Liu, 2002a: Study on modal variation of subtropical high and its mechanism during seasonal transition. Part I: Climatological features of subtropical high structure. *Acta Meteor. Sin.,* **60,** 400–408.

——, ——, and ——, 2002b: Study on modal variation of subtropical high and its mechanism during seasonal transition. Part II: Seasonal transition index over Asian monsoon region. *Acta Meteor. Sin.,* **60,** 409–420.

Nitta, T., 1983: Observational study of heat sources over the eastern Tibetan Plateau during the summer monsoon. *J. Meteor. Soc. Japan,* **61,** 590–605.

Queney, P., 1948: The problem of air flow over mountains: A summary of theoretical studies. *Bull. Amer. Meteor. Soc.,* **29,** 16–29.

Rodwell, M. R., and B. J. Hoskins, 1996: Monsoons and the dynamics of deserts. *Quart. J. Roy. Meteor. Soc.,* **122,** 1385–1404.

Shen, Z., D. Weng, and S. Pan, 1984: An outline of the Qinghai-Xizang Plateau heat source observation experiment. *Collected Papers on the Qinghai-Xizang Plateau Meteorological Experiment (I)* (in Chinese), Science Press, 1–9.

Shi, G. Y., 1981: An accurate calculation and representation of the infrared transmission function of the atmospheric constitutes. Ph.D. dissertation, Tohoku University of Japan, 191 pp.

Shi, L., and E. A. Smith, 1992: Surface forcing of the infrared cooling profile over the Tibetan Plateau. Part II: Cooling-rate variation over large-scale plateau domain during summer monsoon transition. *J. Atmos. Sci.,* **49,** 823–844.

Slingo, J. M., 1987: The development and verification of a cloud prediction scheme for the ECMWF model. *Quart. J. Roy. Meteor. Soc.,* **113,** 899–927.

Smith, E. A., and L. Shi, 1992: Surface forcing of the infrared cooling profile over the Tibetan Plateau. Part I: Influence of relative longwave radiative hearing at high altitude. *J. Atmos. Sci.,* **49,** 805–822.

Tanaka, K., H. Ishikawa, T. Hayashi, I. Tamagawa, and Y. Ma, 2001: Surface energy budget at Amdo on the Tibetan Plateau using GAME/Tibet IOP98 data. *J. Meteor. Soc. Japan,* **79,** 505–517.

Tao, S. Y., 1980: *Torrential Rain in China.* Chinese Meteorology Press, 225 pp.

——, and L. Chen, 1987: A review of recent research on the East Asian summer monsoon in China. *Monsoon Meteorology,* C. P. Chang and T. N. Krishnamurti, Eds., Oxford University Press, 60–92.

Tian, S. F., and T. Yasunari, 1998: Climatological aspects and mechanism of spring persistent rains over central China. *J. Meteor. Soc. Japan,* **76,** 57–71.

Trenberth, K. E., and C. J. Guillemot, 1998: Evaluation of the atmospheric moisture and hydrological cycle in the NCEP/NCAR reanalyses. *Climate Dyn.,* **14,** 213–231.

Wan, R. J., and G. X. Wu, 2007: Mechanism of the spring persistent rains over southeastern China. *Sci. China, Ser. D,* **50,** 130–144.

Wang, B., and LinHo, 2002: Rainy seasons of the Asian–Pacific summer monsoon. *J. Climate,* **15,** 386–398.

Wang, Z. Z., G. X. Wu, T. W. Wu, and R. C. Yu, 2004: Simulation of Asian monsoon seasonal variations with climate model R42L9/LASG. *Adv. Atmos. Sci.,* **21,** 879–889.

Webster, P. J., V. O. Magana, T. N. Palmer, J. Shukla, R. A. Tomas, M. Yanai, and T. Yasunari, 1998: Monsoons: Processes, predictability, and the prospects for prediction. *J. Geophys. Res.,* **103,** 14 451–14 510.

Wu, G. X., 2004: Recent progress in the study of the Qinghai-Xizhang Plateau climate dynamics in China. *Quart. Sci.,* **24,** 1–9.

——, and Y. S. Zhang, 1998: Tibetan Plateau forcing and the timing of the monsoon onset over South Asia and the South China Sea. *Mon. Wea. Rev.,* **126,** 913–927.

——, and Y. M. Liu, 2000: Thermal adaptation, overshooting, dispersion and subtropical anticyclone. I. Thermal adaptation and overshooting. *Chin. J. Atmos.,* **24,** 433–446.

——, and ——, 2003: Summertime quadruplet heating pattern in the subtropics and the associated atmospheric circulation. *Geophys. Res. Lett.,* **30,** 1201, doi:10.1029/2002GL016209.

——, W. Li, H. Guo, H. Liu, J. Xue, and Z. Wang, 1997a: Sensible heat driven air-pump over the Tibetan Plateau and its impacts on the Asian summer monsoon. *Collections on the Memory of Zhao Jiuzhang,* Y. Duzheng, Ed., Chinese Science Press, 116–126.

——, and Coauthors, 1997b: The LASG global ocean–atmosphere–land system model GOALS/LASG and its simulation study. *Appl. Meteor.,* **8,** 15–28.

——, Y. M. Liu, and P. Liu, 1999: Impacts of spatial differential heating on the formation and variation of the subtropical anticyclone. I. Scale analysis. *Acta Meteor. Sin.,* **57,** 257–263.

——, L. Sun, Y. Liu, H. Liu, S. Sun, and W. Li, 2002: Impacts of land surface processes on summer climate. *Selected Papers of the Fourth Conference on East Asia and Western Pacific Meteorology and Climate,* C.-P. Chang et al., Eds., World Scientific, 64–76.

——, Y. Liu, J. Mao, X. Liu, and W. Li, 2004: Adaptation of the atmospheric circulation to thermal forcing over the Tibetan Plateau. *Observation, Theory and Modeling of Atmospheric Variability: Selected Papers of Nanjing Institute of Meteorology Alumni in Commemoration of Professor Jijia Zhang,* X. Zhu et al., Eds., World Scientific, 92–114.

——, J. Wang, X. Liu, and Y. M. Liu, 2005: Numerical modeling of the influence of Eurasian orography on the atmospheric circulation in different seasons. *Acta Meteor. Sin.,* **63,** 603–612.

Wu, T. W., and Coauthors, 2003: The performance of atmospheric component model R42L9 of GOALS/LASG. *Adv. Atmos. Sci.,* **20,** 726–742.

Xie, P., and P. A. Arkin, 1996: Analyses of global monthly precipitation using gauge observations, satellite estimates, and numerical model predictions. *J. Climate,* **9,** 840–858.

——, and ——, 1998: Global monthly precipitation estimates from satellite-observed outgoing longwave radiation. *J. Climate,* **11,** 137–164.

Xie, S. P., and N. Saiki, 1999: Abrupt onset and slow seasonal evolution of summer monsoon in an idealized GCM simulation. *J. Meteor. Soc. Japan,* **77,** 949–968.

Xue, Y. K., P. J. Sellers, J. L. Kinter, and J. Shukla, 1991: A simplified biosphere model for global climate studies. *J. Climate,* **4,** 345–364.

Yanai, M., and C. Li, 1994: Mechanism of heating and the boundary layer over the Tibetan Plateau. *Mon. Wea. Rev.,* **122,** 305–323.

——, and T. Tomita, 1998: Seasonal and interannual variability of atmospheric heat sources and moisture sinks as determined from NCEP–NCAR reanalysis. *J. Climate,* **11,** 463–482.

——, and G. X. Wu, 2006: Effects of the Tibetan Plateau. *The Asian Monsoon,* B. Wang, Ed., Springer, 513–549.

——, S. Esbensen, and J.-H. Chu, 1973: Determination of bulk properties of tropical cloud clusters from large-scale heat and moisture budgets. *J. Atmos. Sci.,* **30,** 611–627.

——, C. F. Li, and Z. S. Song, 1992: Seasonal heating of the Tibetan Plateau and its effects on the evolution of the Asian summer monsoon. *J. Meteor. Soc. Japan,* **70,** 319–351.

Ye, D. Z., and Y. X. Gao, 1979: *Meteorology of the Qinghai-Xizang Plateau*. Chinese Science Press, 278 pp.

Yeh, T. C., 1950: The circulation of high troposphere over China in winter of 1945–46. *Tellus,* **2,** 173–183.

——, S. W. Luo, and P. C. Chu, 1957: The wind structure and heat balance in the lower troposphere over Tibetan Plateau and its surrounding. *Acta Meteor. Sin.,* **28,** 108–121.

——, S. Y. Tao, and M. T. Li, 1959: The abrupt change of circulation over the Northern Hemisphere during June and October. *The Atmosphere and the Sea in Motion,* B. Bolin, Ed., Rockefeller Institute Press, 249–267.

Zhang, J. J., and Coauthors, 1988: *Advances in the Qinghai-Xizang Plateau Meteorology—The Qinghai-Xizang Meteorology Experiment (QXPMEX, 1979) and Research*. Chinese Science Press, 268 pp.

Zhang, X. H., G. Y. Shi, H. Liu, and Y. Q. Yu, 2000: *IAP Global Ocean–Atmosphere–Land System Model.* Science Press, 252 pp.

Zhou, M., and Coauthors, 2000: *Observational, Analytical, and Dynamic Study of the Atmospheric Boundary Layer of the Tibetan Plateau*. Meteorology Press, 125 pp.